Advances in Radiation Oncology (2024) 9, 101503

advances in radiation oncology

www.advancesradonc.org

Scientific Article

Clinical Viability of an Active Spot Scanning Beam Delivery System With a Newly Developed Carbon-Ion Treatment Planning System

Yixiao Guo, MD,[a] Zhiqiang Liu, MD,[b] Shifang Feng, MD,[a] Hongyi Cai, MD,[a,*] and Qiuning Zhang, PhD[b,*]

[a]*Department of Radiation Oncology, Gansu Provincial Hospital, Lanzhou, P.R. China; and* [b]*Institute of Modern Physics, Chinese Academy of Sciences, Lanzhou, Gansu, P.R. China*

Received 27 July 2023; accepted 19 January 2024

Purpose: Although active spot scanning irradiation technique is theoretically superior to passive-scattered broad beam irradiation with respect to normal tissue sparing, corroborations of the clinical benefit of carbon-ion spot scanning have remained scarce. This study aims to investigate the feasibility and clinical implementation of an active spot scanning beam calculation algorithm in a homemade carbon-ion treatment planning system by comparing it with a conventional passive uniform scanning technique.

Methods and Materials: Carbon-ion plans were initially formulated using spot/uniform scanning methods in 22 participants enrolled in a prospective observational clinical trial. Subsequently, 2 additional plans were designed, resulting in 3 carbon-ion plans for each participant: uniform and spot scanning with miniridge filters of 2 mm and 4 mm, respectively.

Results: The findings revealed no significant differences in dose homogeneity; however, significant differences in dose conformity were found between the active and passive scanning plans. For dose drop-off outside the target volume, the average gradient index values were 1.94 (95% CI, 1.79%-2.09%), 1.87 (95% CI, 1.73%-2.01%), and 3.20 (95% CI, 2.80%-3.61%) for the miniridge filters of 2 mm and 4 mm, and uniform scanning plans, respectively. The pretreatment tumor volume was 124.7 cm^3 (range, 54.2-234 cm^3), and the average shrinkage observed was 38.4% (95% CI, 17.6%-59.4%). Seven participants experienced grade 1 acute toxicity, and 4 experienced grade 2 acute toxicity. However, none of the patients developed grade 3 acute toxicity.

Conclusions: Increasing evidence suggests that potential clinical advantages of spot scanning delivery underlie its technical characteristics. As one among the few institutions currently using carbon-ion radiation therapy, the investigation also provides promising safety and efficacy outcomes from the initial groups of treated participants, thereby contributing to the established clinical evidence supporting the effectiveness and superiority of carbon-ion therapy.

Sources of support: This study was financially supported by the Natural Science Foundation of Gansu province (23JRRA1284, 22JR5RA693). the National Key Research and Development Program of China (Grant No. 2022YFC2401500), Gansu Province Project of Science and Technologies (Grant No. 22CX8JA149), and Science and Technology Project of Lanzhou City (Grant No. 2023-1-9). The funder did not participate in the study's design and manuscript composition.

Requests for research data should be directed to the corresponding author. Data requests from researchers who provide a methodologically sound proposal will be considered up to 36 months from the date of publication.

*Corresponding authors: Hongyi Cai, MD; Email: gschy777@163.com and Qiuning Zhang, PhD; Email: zhangqn@impcas.ac.cn

Introduction

Drawing on technical and clinical investigations performed on carbon-ion therapy at the inaugural heavy-ion facility, the Heavy Ion Research Facility in Lanzhou (HIRFL) concluded its clinical trial for the second domestically produced commercial medical accelerator in China. The therapy terminal at HIRFL is currently equipped with both passive scattering (uniform scanning) and active spot

https://doi.org/10.1016/j.adro.2024.101503

scanning (pencil beam scanning) beamlines. As indicated by previous research,[1-3] there were substantial differences between passive and active scanning beam irradiation in terms of biologic modeling, absorbed dose calculation, and dose delivery. Compared with passive-scattered broad beam irradiation, the active spot scanning beam line has been recently tested and verified, establishing it as a significant advancement in carbon-ion therapy.

In September 2022, the single-period energy variation technique was successfully implemented at the HIRFL therapy terminal, allowing slow extraction of multiple energies within a single period of the synchrotron. This breakthrough achieved >80% extraction efficiency comprehensively, enabling rapid changes in the beam energy for precise irradiation of target tumors. The resulting advancements in the performance of carbon-ion therapy facility and promoting spot-scanning beam techniques using pencil beams with higher efficiencies are significant contributions to clinical applications. The ciPlan carbon-ion treatment planning system (TPS) was developed by the Institute of Modern Physics (IMP), Chinese Academy of Sciences.[3] In 2020, ciPlan TPS was implemented in clinical practice, resulting in the registration of >700 patients for treatment at the first domestically produced carbon-ion beam line located at Wuwei Heavy Ion Center.[4] The patients received treatment through the fixed nozzle treatment, using a conventional passive-scattered irradiation technique with single-beam irradiation, 2-beam opposite irradiation, or 2-beam orthogonal irradiation.[4,5-7]

From October 28, 2022, to January 16, 2023, an independent clinical trial was officially completed at the second homemade carbon-ion therapy facility at HIRFL. Twenty-eight participants were enlisted in the study. Among them, 5 participants were excluded because of extensive distant metastasis, and one voluntarily dropped out of the study. Consequently, 22 participants were included in this clinical trial. They complied with the relevant China Food and Drug Administration regulations and underwent uniform-scanning and spot scanning carbon-ion therapy. Using active spot scanning, the dose conformity was theoretically enhanced, and damage to the organs at risk was minimized. However, few studies have demonstrated this due to the unavailability of carbon ion-equipped centers. The clinical application of carbon ion spot scanning plans has been subjected to limited investigations, and it is imperative to carefully evaluate the potential benefits of significant improvements. To address this gap, the cases enrolled in the clinical trial were used as a model for the analysis. Specifically, 3 carbon-ion treatment plans were developed for each case, incorporating both spot scanning (miniridge filters [MRF] of 2 mm [MRF2] and 4 mm [MRF4]) and uniform scanning techniques, aiming to examine the dose distribution characteristics of both techniques and assess the feasibility of active beam delivery to establish its clinical efficacy. Furthermore, this investigation has the potential to enhance the comprehension of the achieved dose distribution in treatment plans when transitioning from passive beam delivery to spot scanning dose algorithm.

Methods and Materials

The experimental procedures used in this study were conducted in adherence to pertinent guidelines and regulations, and the informed consent of participants was waived. The Medical Ethics Committee of Gansu Provincial Hospital (B-1802/451-106) has scrutinized and sanctioned this clinical trial.

Patient selection and carbon-ion beams

Twenty-two out of 615 patients met the inclusion criteria and were enrolled in the study. The treatment sites included the head and neck, thorax, abdomen, pelvic region, spine, and limbs, and the types of pathologic tumors are shown in Table E1. Four treatment rooms, each with 5 fixed beam ports and equipped with both active and passive beam nozzles, made up the carbon-ion facility (Table E2). The HIRFL port layouts are shown in Fig. E1. Additional accessories, such as a compensator (Figs. E2-E4), multileaf collimator, and ridge filter (30-120 mm, Fig. E5), are also available.

Target volume definition, design, and evaluation of carbon-ion treatment plans

Fifteen participants underwent conventional axially enhanced scanning with intravenous contrast. A respiratory gating strategy was implemented for moving targets comprising one participant with liver cancer and 6 participants with lung cancer. Contrast-enhanced 4-dimensional (4D) imaging was acquired for these participants. This technique was implemented with caution and consequently, a decision was made to establish a definitive internal target volume (ITV) that encompasses the tumor throughout the respiratory cycle, aiming to encompass the tumor regardless of any uncertainties encountered during the irradiation process. The time window for irradiation was flexibly determined according to the respiratory curves of each participant on each treatment day. A commercial system was used to monitor live breathing cycles through a pressure sensor fastened to a waist belt. A separate ITV was not set for tumors located at the intracranial, limb, sacrum, or sacrococcygeal sites, because they were almost devoid of autonomous movement characteristics. An isotropic margin of 3 to 5 mm was added to the clinical target volume (CTV) to create the planned target volume (PTV).

The ITV was created by adding a 5 mm margin to the gross tumor volume (GTV) in participants planned using 4D computed tomography (CT). To generate the PTV, a margin of 3 to 5 mm was set anteroposteriorly and to the right-left; however, a 5 to 10 mm margin was set craniocaudally from the ITV. In addition, the ratio of CTV/ITV to PTV margins was considered based on tumors adjacent to organs at risk (OARs).

The ciPlan TPS (version 2.0) was used to design the carbon-ion treatment plans, and the prescribed doses ranged from 50 to 70 Gy (relative biological effectiveness [RBE]) in 10 to 20 fractions. Carbon-ion therapy was delivered 5 days a week, and subsequent replanning was performed to generate 3 plans for each participant containing both spot scanning (using 2 mm and 4 mm MRFs to broaden the single-energy Bragg peak) and one uniform scanning plan. Robust optimization primarily considers the uncertainties of the treatment setup and carbon-ion beam range by expanding the PTV to obtain PTV_Expanding. Based on the properties of the carbon-ion beam used in the HIRFL therapy terminal and the potential for dose calculation uncertainty by ciPlan TPS, a PTV expansion along each beam direction is routinely performed at 3.5% of the prescribed range with an additional 3 mm as a range margin in depth (relative to the proximal and distal tumor surfaces), which is the same as the Roberts Proton Therapy Center.[8] In some cases, this value may need to be adjusted based on beam orientation, patient geometry, and location of OAR in relation to the tumor volume. Robust optimization also incorporates beam direction selection. The beam direction is selected with the least number of organs at risk and the least amount of range uncertainty or organ motion. After dose calculation, all carbon-ion plans covered at least 95% of the PTV with the prescribed dose by optimizing PTV_Expanding. Cumulative dose-volume histograms (DVHs) were computed for each plan to assess the dosimetric and radiobiological parameters.

To fulfill the ciPlan beam modeling requirements, the layer thickness of the spot scanning plan was set to 4 mm, spot spacing to 2 mm, and grid size of both scanning techniques was set to 2 mm × 2 mm × 2 mm. For each plan, a consistent beam entrance strategy involving 2 or 3 beam ports was used and 3 carbon-ion plans with comparable target coverages were generated for each target volume to examine the impact of the beam delivery technique on the OAR dose. A range of dosimetric parameters were used as endpoints to quantify the target coverage and dose distribution. These include the homogeneity index (HI), conformity index (CI), and gradient index (GI).

HI was determined as follows[9,10]

$$HI = \frac{D_{5\%}}{D_{95\%}} \quad (1)$$

where, $D_{5\%}$ and $D_{95\%}$ are the minimum doses encompassing 5% and 95% of the target volume, respectively. It assesses the uniformity of dose distribution across the target volume. An HI value closer to 1 indicates superior dose uniformity, with an acceptable range between 1.00 and 1.40.[9,10]

CI was calculated by[9,11]

$$CI = \frac{V_{RI}}{TV} \quad (2)$$

where, V_{RI} is the volume of the reference isodose,[9,11] 95% of the prescribed dose was used here as the reference isodose, and TV is the target volume. CI refers to the degree of prescribed dose conformity with the target volume, and it is desirable that the CI remains close to 1.[9,11]

GI is used to evaluate dose attenuation outside the target volume,[12] where $PIV_{1/2}$ and PIV represent the volume encompassed by 50% of the prescribed isodose line and the prescribed isodose line, respectively.

$$GI = \frac{PIV_{1/2}}{PIV} \quad (3)$$

As the GI value decreases, the dose attenuation outside the target increases steeply compared with the inverse square law.[13]

To ensure an equitable comparison, 3 plans were standardized for each participant based on identical dosimetric criteria, specifically the $D_{95\%}$ of the PTV. Dose constraints were determined by referring to multi-institutional research at Japanese proton beam facilities (Table E3). The maximum (D_{max}) and mean (D_{mean}) doses were assessed for both PTV and PTV_Expanding. A set of appropriate V_x values (x range, 18-70), D_{mean}, D_{max}, and dose-volume parameters, including D_2, D_5, and D_{10}, represent the minimum dose received by 2%, 5%, and 10% of the OAR, respectively. V_x was the percentage volume of an OAR receiving a dose of x or more.

Follow-up and toxicity evaluation

All participants were followed up prospectively. Toxicities that occurred within 3 months of treatment initiation were categorized as acute adverse events. Observed toxicity was categorized according to the criteria of Common Terminology Criteria for Adverse Events (CTCAE, version 5.0) and Radiation Therapy Oncology Group/European Organization for Research and Treatment of Cancer. CT and/or magnetic resonance imaging (MRI) scans were performed to check for lung reactions and tumor size, and the largest and smallest tumor diameters were measured on transverse sections. Data regarding skin reactions and other physical symptoms were collected through interviews and inspection.

Statistical analysis

All statistical tests were performed using GraphPad Prism software (version 9.1) to assess the statistical

significance of dosimetric parameters between spot scanning, uniform scanning, and both MRF plans. Additionally, GraphPad Prism software was used to generate figures pertaining to HI, CI, and GI of the target volume as well as the dosimetric parameters of the OAR. The Shapiro-Wilk significance hypothesis was applied to the MRF4, MRF2, and uniform scanning groups, with a test level of $\alpha = 0.05$. A paired t test with Bonferroni correction for multiple testing was used to assess the significance of differences between the distributions of the MRF4 and MRF2 groups, depending on the normality of the data. A 2-tailed Wilcoxon signed-rank test was also performed. Additionally, the independent t test was used for normally distributed data in the MRF4/MRF2 and uniform scanning groups, whereas the nonparametric Mann-Whitney U test was used for nonnormal data. Significance was determined using a 2-tailed P value of less than .05.

Results

Evaluating HI, CI, and GI within the target volume as well as various dose-volume parameters in OAR for the 3 carbon-ion plans

As shown in Fig. 1a and b, the maximum dose of the PTV among the 3 plans was not statistically comparable ($P < .05$), whereas the evaluation of the PTV mean dose

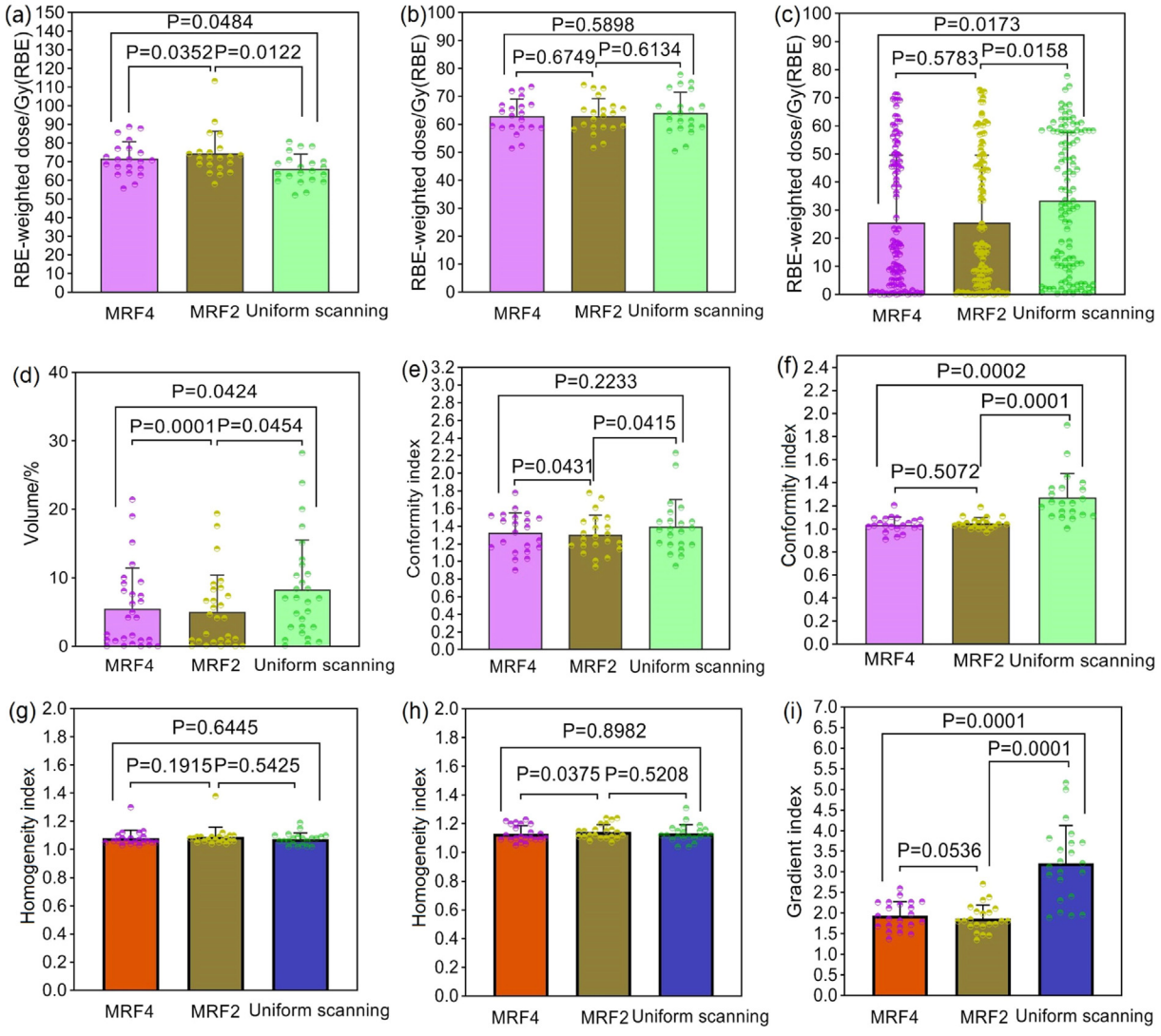

Fig 1 Homogeneity index (HI), conformity index (CI), gradient index (GI), and dosimetric evaluation parameters in miniridge filters 4 mm and 2 mm, and uniform scanning carbon-ion plans. (a) D_{max} in planned target volume (PTV); (b) D_{mean} in PTV; (c) comparison of dose received by various organs at risk; (d) the percentage volume of organs at risk encompassed by a dose of x or more; (e) CI in PTV; (f) CI in PTV_Expanding; (g) HI in PTV; (h) HI in PTV_Expanding; (i) and GI in PTV_Expanding.
Abbreviations: MRF2 = miniridge filters 2 mm; MRF4 = miniridge filters 4 mm; RBE = relative biological effectiveness.

revealed no significant difference ($P > .05$). Figures 1c and d show that the uniform scanning technique resulted in a higher average absolute dose and percentage volume of OAR, and the MRF2 plans exhibited a superior protective effect against OAR compared with the MRF4 plans, albeit with a potential doubling of the treatment time. The results indicated that the dose reduction to multiple OAR was significantly influenced not only by the various beam delivery techniques, but also by the diverse MRFs used in the spot scanning plans. A CI value closer to 1.0, represents a better dose conformity to the target volume, which in turn facilitates the higher dose delivery to the target volume while minimizing damage to the surrounding normal tissue. Notice the CI values of each group in PTV and PTV_Expanding are predominantly concentrated in the ranges of 0.9 to 1.78 and 0.9 to 1.6, among which 2 CI values exceed 2 and 1.8 (Fig. 1e, f), respectively. Within the PTV group, 21, 19, and 21 cases in the MRF4 (mean value, 1.218), MRF2 (mean value, 1.192), and uniform scanning groups (mean value, 1.385), respectively, had CI values greater than 1.0. In the PTV_Expanding group, there were 13, 17, and 19 instances in the MRF4 (mean value, 1.002), MRF2 (mean value, 1.017), and uniformly scanned (mean value, 1.196) groups, where the CI values exceeded 1.0. Outliers were exclusively observed within groups using uniform scanning plans. As shown in Fig. 1g and h, the dose homogeneities within the TVs generated by the spot scanning modality were comparable to those achieved using uniform scanning modality ($P > .05$). Notably, a larger GI value corresponded to a greater degree of dose spillage outside the target volume. Consequently, the spot scanning technique effectively minimized excessive dosing in the proximal region of the target, after the cessation of the beam supply (as depicted in Fig. 1i).

Case Presentation

Case 1 pancreatic head carcinoma

Figure 2 depicts the case of a 39-year-old male patient diagnosed with local primary pancreatic head carcinoma measuring a maximum of 3.5 cm in diameter, located at the right anterior superior segment, near the spinal cord. Because of the colon's proximity to the PTV, a 1 mm margin was excluded from the right side of the PTV during expansion to form PTV_Expanding.

For pancreatic head carcinoma, typical dose distributions were generated using spot and uniform scanning techniques as shown in Fig. 3. The total dose administered was 53.2 Gy (RBE) through 3 portals, delivered in 13 fractions, with 4.0 Gy (RBE) in 10 fractions for PTV and 4.4 Gy (RBE) in 3 fractions for primary gross tumor volume. The major OAR that are in close proximity to the PTV include the colon, small intestine, stomach, right kidney, and spinal cord. Based on the tumor location, a combination of one anterior and 2 lateral-opposing portals (dose

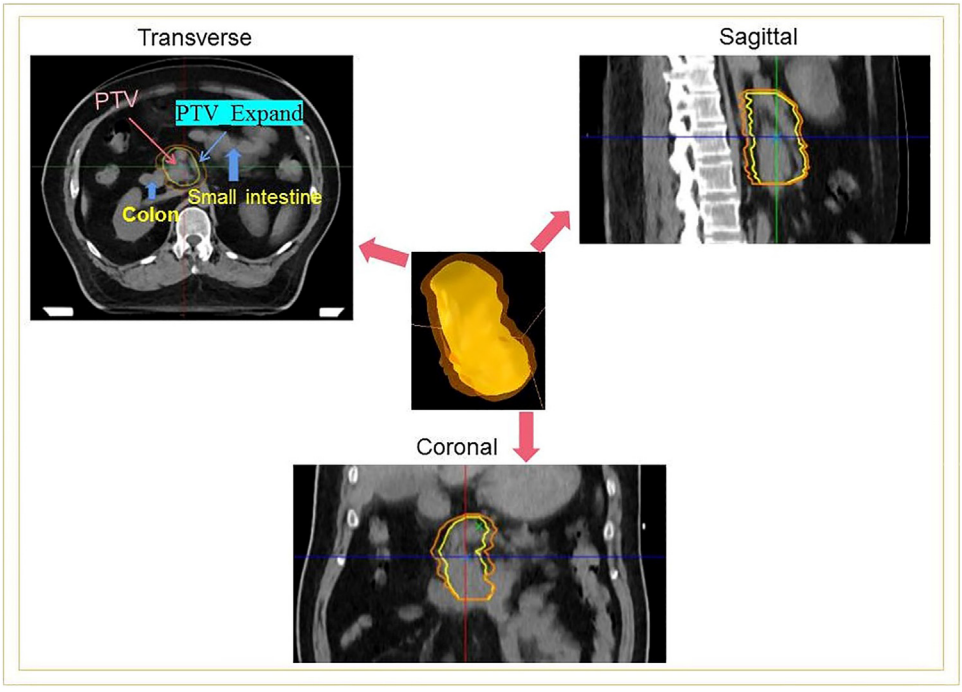

Fig 2 Planned target volume expanding view in transverse, sagittal, coronal, and beam's eye view of the pancreatic head carcinoma. An abdominal computed tomography scan revealed a tumor mass in contact with the colon.
Abbreviation: PTV = planned target volume.

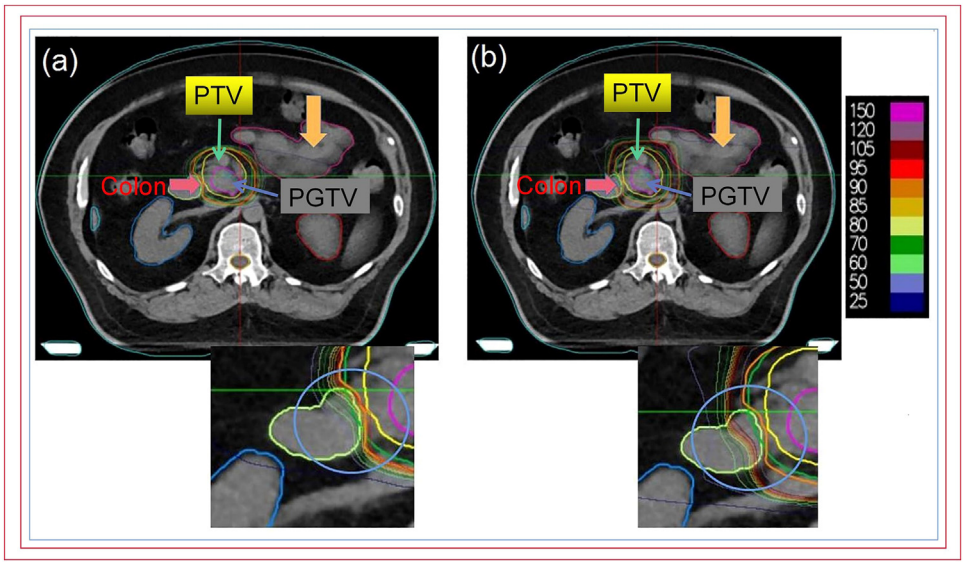

Fig 3 The dose distributions of spot scanning and uniform scanning irradiation in the left and right panels, respectively. (a) Spot scanning mode; and (b) uniform scanning mode. Colors indicate the shape and magnitude of various isodose lines.
Abbreviations: PGTV = primary gross tumor volume; PTV = planned target volume.

ratio 1:1:1) was used to deliver the beams in the supine position. The PTV was defined to encompass a 0.5 cm margin around CTV, except on the right side, where the margin was narrower to prevent the colon from being exposed to the high-dose region. The spot-scanning beam technique produced varying dose lines, as evidenced by the proximity of the high-dose lines to the tumor target volume within the blue circle. Following the preceding stage, it is feasible to administer a substantial dose to the target volume while simultaneously safeguarding the OAR susceptible to the high-dose region of the carbon ion beam, specifically the colon.

The dose-volume histograms generated for the PTV and OAR depicted in Fig. 4 indicate that the OARs were exposed to significantly lower levels of radiation in the low-medium dose range in the spot scanning plan compared with the uniform scanning plan. This disparity has potential significance in reducing treatment-related complications, particularly the risk of gastrointestinal bleeding, ulceration, necrosis, and perforation.

Case 2 chordoma of the skull base

A 38-year-old man presented with a tumor in the nasal septum. An incisional biopsy revealed the presence of a chordoma in the skull base. An MRI T1-weighted image was used to determine the GTV, after CT/MRI fusion. Note that the margin toward the brain stem was reduced to comply with the dose constraints. The active spot scanning technique delivered a total dose of 60.8 Gy (RBE), in 3.8 Gy (RBE)/fraction. The treatment plan comprised 2 horizontal ports that traversed the shortest normal tissue, and a vertical beam direction was avoided to prevent the beam dose from falling off in front of the brain stem. In the event of a small setup error, the beam directed toward the nasal septum may inadvertently reach the brain stem.

As shown in Fig. 5, the representative dose distributions from the 3 carbon ion plans exhibited a low-dose region that followed the beam path, with a rapid decrease in the out-of-target dose in the anterior and posterior directions. Furthermore, the equivalent uniform dose delivered to adjacent normal tissues was greater in the uniform scanning mode (Fig. 5c). The D_5 and D_{mean} values were marginally elevated in the uniform scanning plans, as shown in Table E4, despite 95% of the PTV receiving the same treatment dose. Additionally, the horizontal uniform scanning mode resulted in higher doses of certain OAR as indicated in Table E5.

The spot scanning delivery technique leads to tumor regression

If there was an increase in the tumor size between pretreatment and the follow-up MRI images, the participants were scored based on tumor progression. Conversely, if the tumor was maintained or decreased in volume, the patient was considered to have achieved tumor control. The volumetric analysis revealed that all participants, except one, experienced tumor shrinkage compared with their pretreatment volume. The mean pretreatment tumor volume was 124.7 cm^3 (range, 54.2-234 cm^3), and the average tumor volume shrinkage rate was 38.4% (range, 17.6%-59.4%).

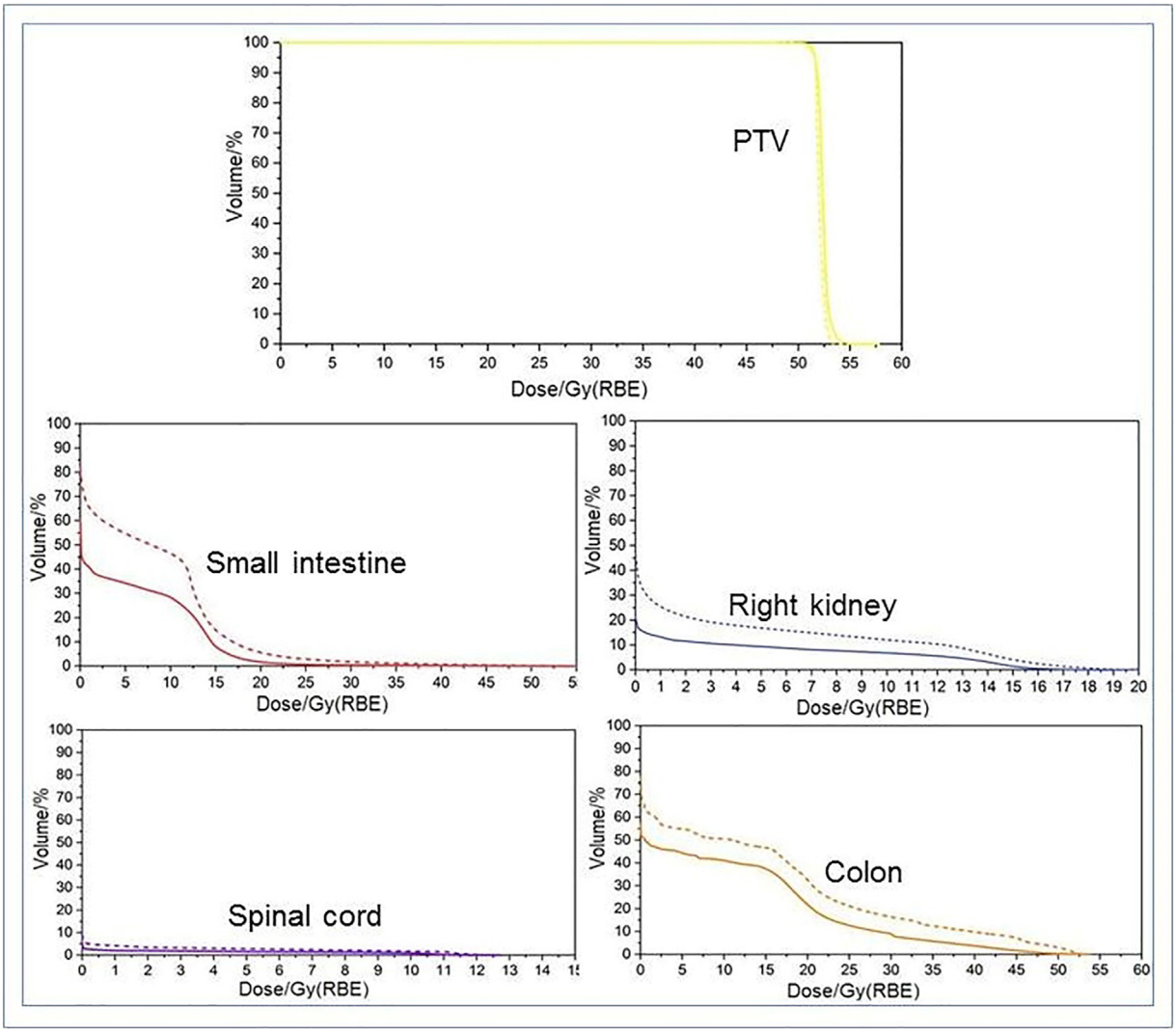

Fig 4 Dose-volume histogram comparison of the planned target volume and organs at risk in patients with pancreatic head carcinoma. The solid and dotted lines, which are both the same color, correspond to spot scanning and uniform scanning plans, respectively.
Abbreviations: PTV = planned target volume; RBE = relative biological effectiveness.

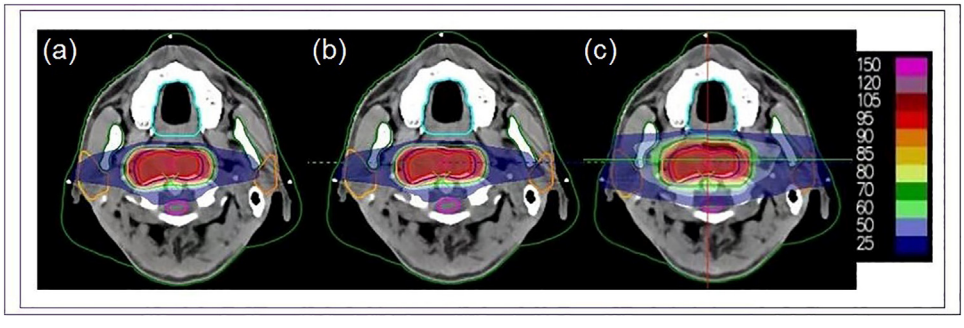

Fig 5 Dose distributions in transverse view with isodose lines for 3 carbon-ion plans in the chordoma case. A fixed horizontal line and rotation of the couch were used to deliver 2 opposed lateral portals. (a) Miniridge filters 4 mm spot scanning plan; (b) miniridge filters 2 mm spot scanning plan; and (c) uniform scanning plan. The results indicate a higher concentration of high-dose area in the target volume. The colors of the isodose lines represent the shape and magnitude of the respective doses.

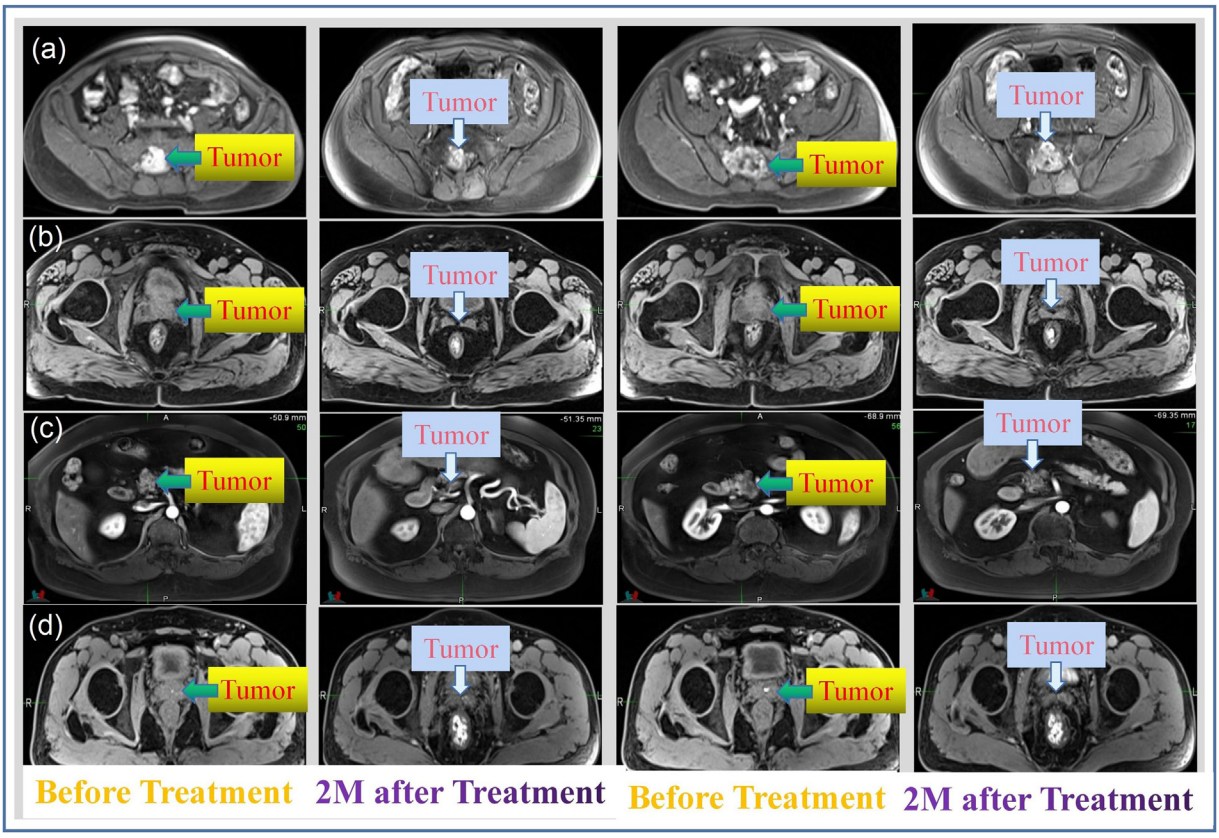

Fig 6 Four participants underwent magnetic resonance imaging scanning 2 months after spot scanning delivery. (a) Schwannoma at sacrum case; (b) prostate cancer case; (c) pancreatic head carcinoma case; and (d) prostate cancer case. The tumors exhibited significant regression, and no adverse effects such as bleeding, ulceration, necrosis, or perforation of the small intestine were observed after treatment.

Figure 6 depicts the volumetric progression of 4 participants before and after treatment using spot-scanning carbon ion plans. A significant decrease in tumor volume and weakened MRI signal intensity within the tumor sites were observed over time using in vivo MRI.

Toxicities

The median follow-up duration from the initial carbon-ion radiation therapy was 2.6 months (range, 2-3 months). The overall treatment tolerance was good, and all participants completed the planned therapy schedule. In terms of acute toxicities, adverse effects were mainly grades 1 and 2. The observed toxicities are presented in Table 1. Three participants (100%) developed grade 1 acute mucositis, 3 (60%) developed grade 2 acute dermatitis, and 2 (100%) developed grade 1 acute dermatitis. During radiation therapy and the present follow-up period, no grade 3 or higher device-related acute adverse effects occurred. Therefore, overall safety was good. In these cases, the probability of adverse effects was predictable and occurred only on the affected side, and carbon-ion radiation therapy was performed with sufficient informed consent before treatment.

Discussion

Between October 28, 2022, and January 16, 2023, a clinical trial of carbon-ion therapy was conducted by HIRFL and Gansu Provincial Hospital to validate the safety of carbon-ion radiation therapy and assess its efficacy as a present therapy terminal for antitumor effects. A carefully selected group of patients with local primary and recurrent cancers was formally enrolled and subjected to uniform or spot-scanning deliveries. To ensure an equitable dosimetric comparison, MRF2, MRF4, and uniform scanning plans were devised for each participant with comparable target dose coverage. The results indicate that the spot scanning technique exhibited a similar dose homogeneity to the target volume corresponding to the conventional uniform scanning techniques (Fig. 1g, h). As anticipated, spot scanning plans have the potential to achieve superior dose conformity compared with uniform scanning plans (Fig. 1e, $P = .0415$, $P = .2233$; Fig. 1f, $P = .0001$, $P = .0002$). Because

Table 1 Toxicities after carbon ion radiation therapy

AE	Clinical diagnosis	Participant no.	Incidence	Dose/fraction
Acute mucotitis (grade 1, %)	Prostate cancer	3	3 (100%)	57.6 Gy (RBE)/16F
Acute dermatitis (%)				
Grade 1	Chondrosarcomas	2	2 (100%)	70 Gy (RBE)/16F
	Sacrum metastatic carcinoma	1	0 (0%)	50 Gy (RBE)/10F
Grade 2	Sacrum chordoma, schwannoma	5	3 (60%)	69-70 Gy (RBE)/15-16F
Radiation pneumonitis (%)	Lung cancer	6	0 (0%)	57-63 Gy (RBE)/10-12F
-	Recurrent nasopharyngeal carcinoma	2	0 (0%)	54-60 Gy (RBE)/18-19F
Abnormal electrocardiogram (grade 1, %)	Cranial chordoma	1	1 (100%)	60.8 Gy (RBE)/16F
Digestive system (grade 2, %)	Pancreatic cancer	1	1 (100%)	57.6 Gy (RBE)/14F
Hematology (grade 1, %)	Liver cancer	1	1 (100%)	65 Gy (RBE)/10 F

Abbreviations: AE = adverse event; RBE = relative biological effectiveness.

the PTV_Expanding was optimized to achieve a prescription dose coverage of at least 95% of PTV, the dose conformity of PTV_Expanding (Fig. 1f) could more accurately reflect the fact that the spot scanning technique increased conformity to the target volume and modulated the dose more flexibly than the passive uniform scanning technique. Additionally, spot scanning plans exhibit a sharper dose fall-off in the out-of-target volume, resulting in a smaller GI value. This suggests a reduced intermediate dose around the PTV and a lower incidence of toxicity in the surrounding normal tissue. The sparing OAR assessment revealed that spot-scanning delivery effectively decreased the average dose and volume above the threshold for OAR, particularly those in close proximity to the target volume. These findings demonstrate that the active beam delivery technique used in the domestic ciPlan carbon-ion TPS satisfies the clinical demands for dose modulation and RBE optimization and exhibits superior dosimetry characteristics compared with the uniform scanning mode. After undergoing spot scanning carbon-ion radiation therapy, the follow-up MRI performed 2 months later revealed a 38.4% average reduction in tumor volume from the initial size. Throughout the follow-up period, all tumor volumes gradually decreased without any transient volume expansion. The observed toxicities showed that no participant suffered grade 3 or higher acute adverse effects within 3 months after treatment initiation.

The delayed availability of spot scanning carbon-ion beam delivery in China can be attributed to the complex technological requirements necessary for the rapid and secure implementation of pencil beam scanning in clinical settings.[14] The construction of a passively scattered carbon-ion beam line is a nontrivial task in itself, and the introduction of spot scanning presents novel challenges in both beam transport and hardware delivery (such as magnets) and software, including treatment control and safety systems, which must be capable of constantly adjusting and verifying beam properties on a millisecond time scale.[15] When establishing the technical prerequisites for a spot scanning-centered facility, particular inquiries necessitate a compromise between conflicting needs. For example, it is essential to consider that effective field abutment necessitates the use of appropriate planning techniques, which may not be universally available in all treatment planning systems. Furthermore, a critical assessment of the pencil beam scanning efficiency involves the ability of the ion beam delivery system to precisely position the spots in absolute terms, rather than solely in relation to one another.

The initial stages of spot scanning focused on achieving the smallest spot sizes, leading to stringent beam property requirements, and small-spot scanning usually requires smaller spot spacing.[16] Previous studies suggested that if the spot size was very small, spot spacing is generally 1.0 to 1.5 times the spot size (1 sigma) in the patient.[17,18] For the homemade carbon-ion facility, the minimum sigma value is 2 mm, the minimum full-width half-maximum is 4.7 mm, and spot spacing should be less than 3 mm. For carbon-ion spot scanning therapy, the intensity control of a scanning system should compensate for delivery errors from one point to another, which can be achieved by narrow spot spacing, for example, ~2 mm.[19] A small spot spacing of 2.5 mm may emerge as a preferred treatment method in proton pencil beam scanning treatment plans.[16,20,21] Because carbon-ion beams have smaller spot sizes than proton beams,[22] 2 mm spot spacing was selected for all energies to avoid mistakes. Despite the potential for a longer field delivery duration in small spot spacing cases compared with large spot spacing, the extended delivery time may introduce greater randomization. Consequently, it can provide the planning system with more freedom to compensate for heightened sensitivity to uncertainties. This, in turn, contributes to enhanced robustness in target coverage and makes the plans less susceptible to interplay effects.[16,23,24]

Synchrotron-based active spot scanning is extremely complex and susceptible to tumor movement, which could result in dose-delivery errors due to the interplay effect.[25] The primary factor limiting the application of scanning techniques in tumor treatments is the susceptibility to errors caused by organ motion. Consequently, only tumors that are effectively immobilized, such as those situated in the head and neck, spinal cord, and lower pelvis, and exhibiting a movement of less than 5 mm, have been subjected to spot scanning modality.[26] In clinical trials, the spot scanning technique has been applied to lesions with minimal motion caused by respiration, such as prostate cancer and chordoma, whereas the uniform scanning technique has been used in parotid gland cancer, upper and lower limb malignancies, and lung cancer. Although treating large irregular target volumes that exhibit significant variations in their thickest and thinnest depths, it is necessary to retract the high-dose region to prevent excessive dosage to distal critical structures, whereas the target volumes with thicker depths will be underdose or cover the target volume with the thickest depth but overdose critical structures.[26] Therefore, the uniform scanning technique may not be optimal for tumors exhibiting complex target shapes and anatomic features, such as lesions that are curved around critical structures.

Conclusion

The evidence available for the effectiveness of carbon-ion radiation therapy is inadequate. This study demonstrated the promising outcomes of carbon-ion radiation therapy in patients with primary tumors and metastases, with acceptable toxicity. A subset of the spot scanning technique is presented and compared with uniform scanning techniques. These are merely the superficial examples in the verification of the antitumor efficacy of carbon ions. The development of advanced carbon ion radiation therapy techniques require collaboration and teamwork. The central theme of this study and the prevailing paradigm in the field are the need for interdisciplinary science and acquiring skills to address the challenges associated with carbon ion rotation gantries, noncoplanar irradiation, and automatic planning technology.

Disclosures

All authors declare no competing interests.

Acknowledgments

We thank each participant enrolled in the clinical trial; members of the trial steering committee; the recruiting center (Gansu Provincial Hospital, PR. China); independent lay members.

Supplementary materials

Supplementary material associated with this article can be found in the online version at doi:10.1016/j.adro.2024.101503.

References

1. Hirohiko T, Tadashi K, Toshiyuki S, et al. *Carbon-Ion Radiotherapy. Principles, Practices, and Treatment Planning*. Tokyo: Springer; 2014.
2. Liu XG, Li Q, Dai ZY. Method of dose calculation for heavy-ion cancer therapy at IMP. *Nucl Phys Rev*. 2009;26:69-75.
3. Nobuteru K, Yoshiki K, Takahiro O, et al. Skin dose reduction by layer-stacking irradiation in carbon ion radiotherapy for parotid tumors. *Front Oncol*. 2020;10:1396.
4. Alshaikhi J, Doolan PJ, D'Souza D, et al. Impact of varying planning parameters on proton pencil beam scanning dose distributions in four commercial treatment planning systems. *Med Phys*. 2019;46:1150-1162.
5. Yang X, Chen H, Chen J, et al. Application status and development trends of medical proton and heavy ionaccelerators. *Chin J Med Instr*. 2019;43:37-42.
6. Wang ZH, Kou HR, Ma XY, et al. Dosimetric comparison of two-dimensional heavy ion treatment plan versus RapidArc treatment plan in the treatment of multiple brain metastases. *J Precis Med*. 2022;37:99-104.
7. Kong L, Wu J, Gao J, et al. Particle radiation therapy in the management of malignant glioma: Early experience at the Shanghai Proton and Heavy Ion Center. *Cancer*. 2020;126:2802-2810.
8. Paganetti Harald. Range uncertainties in proton therapy and the role of Monte Carlo simulations. *Phys Med Biol*. 2012;57:R99-R117.
9. Chen XH, Kuan HL, Shan YW, et al. Planning evaluation of a novel volumebased algorithm for personalized optimization of lung dose in VMAT for esophageal cancer. *Sci Rep*. 2022;12:2513.
10. Kataria T, Sharma K, Subramani V, et al. Homogeneity Index: An objective tool for assessment of conformal radiation treatments. *J Med Phys*. 2012;37:207-213.
11. Feuvret L, Noël G, Mazeron JJ, et al. Conformity index: A review. *Int J Radiat Oncol Biol Phys*. 2006;64:333-342.
12. Chagas Saraiva CW, Cardoso SC, Groppo DP, et al. Gamma Knife radiosurgery for vestibular schwannomas: Evaluation of planning using the sphericity degree of the target volume. *PLoS One*. 2020;15:e0225638.
13. Damodar P, Justin V, Lana S. A novel and clinically useful dynamic conformal arc (DCA)-based VMAT planning technique for lung SBRT. *J Appl Clin Med Phys*. 2020;21:29-38.
14. Noda K. Beam delivery method for carbon-ion radiotherapy with the heavy-ion medical accelerator in Chiba. *Int J Part Ther*. 2016;2:481-489.
15. Johnson JE, Herman MG, Kruse JJ. Optimization of motion management parameters in a synchrotron-based spot scanning system. *J Appl Clin Med Phys*. 2019;20:69-77.
16. Liu CB, Schild SE, Chang JY, et al. Impact of spot size and spacing on the quality of robustly optimized intensity modulated proton therapy plans for lung cancer. *Int J Radiat Oncol Biol Phys*. 2018;101:479-489.
17. Zhu XR, Poenisch F, Li H, et al. A single-field integrated boost treatment planning technique for spot scanning proton therapy. *Radiat Oncol*. 2014;9:202.
18. Tasson A, Laack NN, Beltran C. Clinical implementation of robust optimization for craniospinal irradiation. *Cancers (Basel)*. 2018;10:7.
19. Gemmel A, Hasch B, Ellerbrock M, et al. Biological dose optimization with multiple ion fields. *Phys Med Biol*. 2008;53:6991-7012.

20. Lin HB, Shi CY, Huang S, et al. Applications of various range shifters for proton pencil beam scanning radiotherapy. *Radiat Oncol*. 2021;16:146.
21. Kang M, Hasan S, Press RH, et al. Using patient-specific bolus for pencil beam scanning proton treatment of periorbital disease. *J Appl Clin Med Phys*. 2021;22:203-209.
22. Zhao J, Chen Z, Wu X, et al. Study of an online plan verification method and the sensitivity of plan delivery accuracy to different beam parameter errors in proton and carbon ion radiotherapy. *Front Oncol*. 2021;11: 666141.
23. Liu W, Schild SE, Chang JY, et al. Exploratory study of 4D versus 3D robust optimization in intensity modulated proton therapy for lung cancer. *Int J Radiat Oncol Biol Phys*. 2016;95:523-533.
24. Bert C, Grozinger SO, Rietzel E. Quantification of interplay effects of scanned particle beams and moving targets. *Phys Med Biol*. 2008;53:2253-2265.
25. Park JM, Kim JI, Wu HG. Technological advances in charged-particle therapy. *Cancer Res Treat*. 2021;53:635-640.
26. Liu H, Chang JY. Proton therapy in clinical practice. *Chin J Cancer*. 2011;30:315-326.